Petroleum Science 20 (2023) 600–610

Contents lists available at ScienceDirect

Petroleum Science

journal homepage: www.keaipublishing.com/en/journals/petroleum-science

Original Paper

Nanofluid based on 1-dodecylpyridinium chloride for enhanced oil recovery

Akram Al-Asadi [a, b], Alba Somoza [a], Alberto Arce [c], Eva Rodil [a], Ana Soto [a, *]

[a] CRETUS. Department of Chemical Engineering, Universidade de Santiago de Compostela, E-15782, Santiago de Compostela, Spain
[b] Chemical and Petrochemical Techniques Eng. Department, Basra Engineering Technical College, Sothern Technical University, Ministry of Higher Education and Scientific Research, Iraq
[c] School of Engineering, Universidade de A Coruña, E-15403, Ferrol, Spain

ARTICLE INFO

Article history:
Received 24 November 2021
Received in revised form
1 April 2022
Accepted 16 August 2022
Available online 19 August 2022

Edited by Jia-Jia Fei

Keywords:
Nanofluid
Viscosity
Interfacial tension
Adsorption
Wettability
EOR

ABSTRACT

The use of nanoparticles is considered promising for enhanced oil recovery (EOR), especially when they are combined with surfactants. However, the combination of nano-sized material with surface-active ionic liquids (SAILs) is an unexplored EOR method. In this work, the advantages of mixing Al_2O_3 nanoparticles with the SAIL 1-dodecylpyridinium chloride were investigated. Stable nanofluids in brine could only be achieved using the polymer polyvinylpyrrolidone (PVP) as a stabilizing agent. It was found that the addition of nanoparticles (and PVP) to the surfactant formulation helped to: slightly increase its viscosity, enhance its water-oil interfacial tension (IFT) reduction capacity, and reduce the adsorption on carbonate rocks (adsorption on sandstone was found to be excessive). IFT was selected as target property to minimize for the design of EOR formulations. Core flooding tests were carried out with surfactant (0.5 wt% [C_{12}py]Cl), surfactant-polymer (0.5 wt% [C_{12}py]Cl, 1.0 wt% PVP) and nanofluid (0.05 wt% Al_2O_3, 1.0 wt% PVP, 0.5 wt% [C_{12}py]Cl) formulations in brine (0.5 wt% NaCl). Additional oil recoveries of 3.4%, 7.4% and 12.0% OOIP were achieved, respectively, the nanofluid formulation being the most promising for the application. Moreover, it was found capable of changing the wettability of carbonate rocks from oil-wet to intermediate-wet. The significance of this work lies in showing the new possibilities resulting from the combination of SAILs and nanoparticles for EOR, specifically the combination of [C_{12}py]Cl with Al_2O_3.

1. Introduction

As the secondary oil recovery technique, the injection of water cannot recover more than a third of the original oil from either sandstone or carbonate reservoirs (Sheng, 2011). The interfacial tension (IFT) between water and oil has to be greatly reduced in order to increase the capillary number and enhance the residual oil recovery. This can be carried out using a surfactant that creates a transient microemulsion phase by solubilizing both the water and the oil. It is also known that surfactants can also change rock wettability towards water-wet (Somasundaran and Zhang, 2006; Hirasaki et al., 2011; Sheng, 2011). Both effects are desired when surface-active agents are used as the basis of chemical enhanced oil recovery (C-EOR).

Future surfactants for EOR purposes, with currently promising results at the laboratory scale, are the surface active ionic liquids (SAILs). In addition to the water/oil IFT reduction, and the capacity to alter the wettability of the reservoir rocks, the promising features of these salts for practical applications are: their tuneability and their stability in harsh conditions (Bin Dahbag et al., 2015; Bera and Belhaj, 2016; Somoza et al., 2022). Hezave et al. (2013) and Zabihi et al. (2019) studied the IFT reduction between water and oil with SAILs based on imidazolium and pyridinium cations. Among the SAILs tested in those works, dodecylpyridinium chloride [C_{12}py]Cl is considered promising due to its significant capacity to reduce water/oil IFT that increased in the presence of NaCl. Another alkylpyridinium SAIL, [C_{18}py]Cl, was proposed as a chemical for EOR by Manshad et al. (2017). A higher capacity to reduce IFT than in the case of [C_8py][Cl] was found, and an intermediate effect on wettability alteration towards water-wet was also shown. The effect of

* Corresponding author.
E-mail address: ana.soto@usc.es (A. Soto).

https://doi.org/10.1016/j.petsci.2022.08.018

wettability alteration on oil recovery was confirmed by means of spontaneous imbibition studies with carbonate rocks.

The use of nanofluids is also a method currently being proposed for EOR (Li et al., 2018; Afolabi, 2019). Disjoining pressure is considered one of the key mechanisms of nano-EOR, the nanoparticles being able to induce the detachment of oil from the rock surface. Metal oxide nanoparticles (SiO_2, ZnO, TiO_2, Fe_2O_3, Al_2O_3, etc.) have been found useful for both IFT reduction and wettability alteration (Li et al., 2018). Moreover, an increase of the injecting formulation's viscosity can be achieved using nanoparticles. This reduces the possibility of adverse mobility ratios and helps EOR. For these reasons, the combination of surfactants and nanoparticles is a C-EOR method worth investigating. However, reservoir salinity affects nanoparticle suspension stability, which is why a stabilizing agent is frequently required when nanoparticles alone or the combination of surfactants and nanoparticles are used in practice. Hendraningrat and Torsæter (2015) studied the performance of several nanoparticles (Al_2O_3, TiO_2, and SiO_2) for EOR purposes in Berea sandstone cores, and the stability of the nanofluid was successfully improved by adding the hydrophilic polymer polyvinylpyrrolidone (PVP) at 1 wt%. Polyacrylamide was proposed for the stabilization of SiO_2 nanofluids (Haruna et al., 2020), also in the presence of the surfactant sodium dodecyl sulfate (Sharma et al., 2015). The use of hydrolyzed polyacrylamide is also suggested to stabilize SiO_2 and Al_2O_3 nanoparticles (Gbadamosi et al., 2019) and N,N0-bis(dimethyltetradecyl)-1,6-hexanediammonium bromide+SiO_2 nanoemulsions (Pal and Mandal, 2020) for EOR purposes.

In this work, the combination of SAILs and nanoparticles for EOR is proposed for the first time. Due to practically unlimited number of SAILs, the design of formulations containing both chemicals offers an innovation that multiplies the possibilities of the application. The SAIL 1-dodecylpyridinium chloride, [C_{12}py]Cl, was selected as surfactant due to its ability to decrease the IFT between water and oil (Hezave et al., 2013) and its liquid character at room conditions. Al_2O_3 nanoparticles were selected due to their common use to design nanofluids for EOR (Hendraningrat and Torsæter, 2015; Li et al., 2018; Gbadamosi et al., 2019). The stability of the nanoparticles in aqueous solutions of the SAIL and in different formulations containing NaCl and PVP, as a stabilizing agent and polymer able to increase the viscosity of the formulation, is studied. Stable nanofluids are characterized in terms of density and viscosity. An optimal formulation for EOR is designed using water/oil IFT as target variable to be minimized. The adsorption of the formulation is tested in sandstone and carbonate rocks. Finally, room-temperature flooding tests in carbonated rocks are carried out in order to study the performance of the formulation. Comparative tests are carried out using the SAIL alone, and the SAIL plus polymer to analyze the increment in recovery due to the use of nanoparticles in the EOR process.

2. Materials and methods

2.1. Materials

Surfactant. The cationic SAIL 1-dodecylpyridinium chloride ([C_{12}py]Cl) was purchased from Merck KGaA (purity > 93 wt%). Its chemical structure is shown in Fig. 1. It was purified under high vacuum (< 1 Pa) while stirred magnetically and heated. The purity was checked by ^{1}H and ^{13}C NMR analysis. Those spectra can be seen in Fig. S1 from Supporting Information (SI).

Nanoparticles. Commercial aluminum oxide nanopowder (Al_2O_3) was purchased from Sigma-Aldrich (< 50 nm particle size). The nanomaterial was structurally characterized by X-ray diffraction (XRD). Diffraction patterns were obtained using an X-ray Philips powder diffractometer (PW 1710) with a Cu-kα X-ray source ($\lambda = 1.54$ Å). As shown in Fig. 2(a), the diffraction peaks correspond

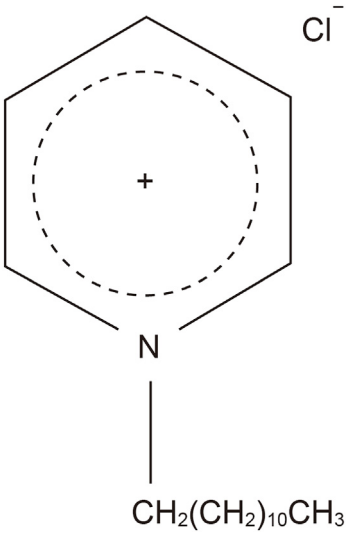

Fig. 1. Chemical structure of 1-dodecylpyridinium chloride.

to the standard card JCPD (Joint Committee on Powder Diffraction Standards) number 29–0063 (Gangwar et al., 2014), indicating the presence of Alumina gamma (derived from boehmite) (γ-Al_2O_3) with tetragonal crystal characteristics. Transmission Electron Microscopy (TEM) was used to determine the shape and size of the nanomaterial, one drop of dispersed nanoparticles in ethanol was deposited on a 400-mesh carbon formvar grid and allowed to evaporate at room temperature. As shown in Fig. 2(b), the dispersed Al_2O_3 nanoparticles have an irregular shape with size distribution between 20 and 50 nm.

Stabilizing agent. Polyvinylpyrrolidone (PVP) with an average molecular weight of 40,000 g/mol was purchased from Sigma-Aldrich.

Crude oil. Crude oil used in this work was kindly supplied by the Repsol refinery plant of A Coruña (Spain) and its main properties are listed in Table 1.

Synthetic brine. Synthetic brines were prepared by dissolving sodium chloride (NaCl) in distilled water. NaCl was purchased from Sigma-Aldrich with ACS reagent purity (≥ 99.0%).

Core samples. Two different types of rock samples were used in this work. Carbonate cores were purchased from Kocurek Industries (Houston) and Berea sandstone cores were supplied by Vinci Technologies (France). Crushed cores were characterized by X-ray powder diffraction using a Bruker D8 Advance (40 kV, 40 mA, theta/theta) equipped with a Cu X-ray tube sealed (CuKα1, $\lambda = 1.5406$ Å), with a LYNXEYE XE-T type detector. Berea Sandstone and carbonate core compositions are shown in Table 2.

2.2. Methods

2.2.1. Nanofluids preparation and characterization

Stock solutions of PVP (4 wt%), [C_{12}py]Cl (4 wt%) and NaCl (10 wt %) in distilled water were prepared by weight in a Mettler Toledo XPE205 analytical balance with a precision of 10^{-4} g. Nanofluids were prepared by mixing a specific amount of Al_2O_3 nanoparticles with distilled water, then adding the required amount of [C_{12}py]Cl stock solution to achieve the desired final surfactant concentration. In the case of nanofluid formulations containing brine, a specific amount of stock solution of stabilizing agent was added to the mixture to obtain a final concentration of 1 wt% PVP, and finally required amounts of NaCl stock solution were added to obtain the desired NaCl concentration. Prepared formulations were stirred

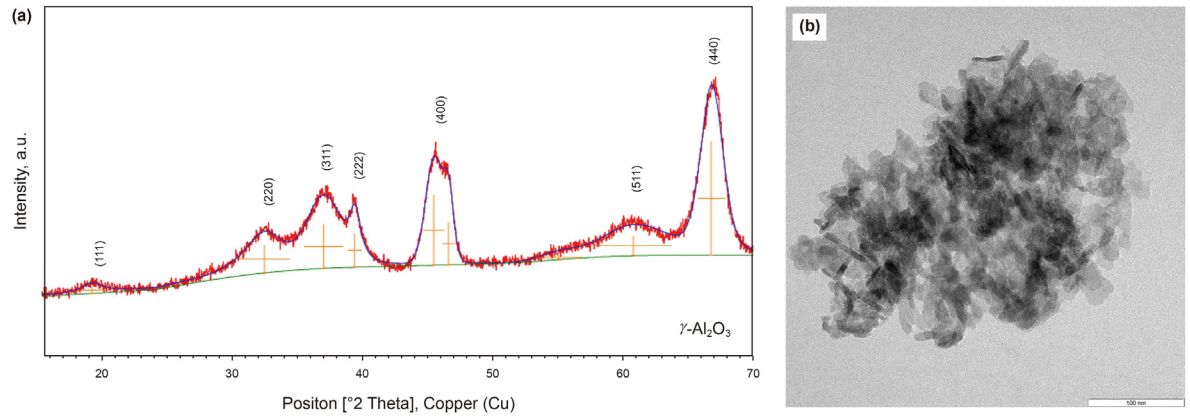

Fig. 2. (**a**) XRD diffraction pattern and (**b**) TEM image of Al_2O_3 nanoparticles.

Table 1
Properties of Repsol crude oil.

Property	Value
Density at 288.15 K, kg/m^3	811.1
API, °	42.9
Reid vapor pressure, kPa	44.9
Viscosity at 293.15 K, kg/m·s	$4.861 \cdot 10^{-3}$
Saturates, wt%	43.5
Aromatics, wt%	41.7
Resins, wt%	11.6
Asphaltenes, wt%	3.2

10 min using a magnetic stirrer, and 5 min with a Bandelin Sonopuls ultrasonic probe with a 10% power and pulsed cycle 1 (0.1 s active interval and 0.9 s passive interval).

Providing a stable nanofluid is one of the major challenges in the application of nanoparticles in EOR. Due to their small particle size, they possess high surface energies that tend to be minimized in the form of aggregates. Those aggregates may lead to pore blocking and alter rock properties, so aggregation must be avoided (Hendraningrat and Torsæter, 2015; Saha et al., 2018; Cacua et al., 2019; Pal et al., 2019; Rostami et al., 2020; Mahmoudpour and Pourafshary, 2021). In the present work, nanofluid stability was analyzed using two techniques: zeta potential measurements and direct visualization. A Zetasizer Nano ZS (Malvern) was used to measure zeta potential. This measurement provides information related to electrical interactions between droplet surfaces. Nanofluids with zeta potential greater than ± 30 mV are generally considered as stable (Choudhary et al., 2017; Saha et al., 2018; Cacua et al., 2019; Pal et al., 2019). However, this method only accounts for electrostatic repulsive interactions and does not account for the steric hindrance effect of the coating assembly (Pal et al., 2019). Thus, additional visualization tests are required. To that aim, nanofluid solution samples were prepared in closed transparent vials and monitored for 7 day at room temperature. Nanofluid samples were considered stable if no precipitation was observed after that time.

Density and viscosity of the prepared nanofluids were simultaneously measured at 298.15 K using an Anton Paar DMA 5000 M oscillating U-tube density meter with an Anton Paar LOVIS 2000 ME micro-viscometer module, based on the rolling ball principle, attached. The Newtonian character of nanofluids was previously confirmed. To that aim, an Anton Paar MCR102 rheometer was used. As example, Fig. S2 shows viscosity as a function of shear rate of the most viscous nanofluid used in this work. All measurements were carried out, at least, twice to guarantee their repeatability.

2.2.2. Dynamic interfacial tension (IFT) measurements

Dynamic IFT between crude oil and the surfactant or nanofluid formulation was measured using a spinning drop tensiometer (Krüss SITE100). The temperature was set to 298.15 K using a Julabo thermostatic bath. Aqueous solutions were sonicated using a Branson 5200 sonication bath for 2 h to ensure that there was no air dissolved in the samples. The capillary tube was filled with the aqueous solution and a drop of 4 μL of crude oil was injected, using a Hamilton Bonaduz Schweiz microliterTM #701 syringe, in the middle of the tube rotating at low speed (60 rpm). Rotating velocities between 5000 and 6000 rpm were then applied to obtain a drop length at least 4 times larger than its diameter. The IFT was calculated according to the Vonnegut equation:

$$IFT = \Delta\rho \cdot \omega^2 \cdot D^3 \Big/ 32 \quad (1)$$

where $\Delta\rho$ is the density difference between the dense and light phases, ω is the angular velocity and D is the diameter of the oil drop. All the experiments were performed at least twice to ensure repeatability.

2.2.3. Adsorption studies

The adsorption determination procedure was implemented based on previous works in the literature (Ahmadi et al., 2012; Ahmadi and Shadizadeh, 2015, 2019; Ahmadi, 2016; Al-Wahaibi et al., 2017). Carbonate or sandstone rocks were crushed into

Table 2
Rocks mineralogy.

Berea Sandstone	Content, %	Carbonate	Content, %
Quartz	79	Calcite	89
Muscovite 2M1	4	Sodium Calcium Pentafluoroaluminate Fluoride – Beta	2
Pentahydroborite	13	Diopside	9
Albite	4		

small parts by a jaw crusher and then sieved (≈0.1–0.5 mm). Several vials were prepared containing 5 mL of the selected formulation and 1 g of crushed rock, and shaken for 3 days in a Selecta Boxcult orbital shaker at 298.15 K. Sampling was carried out from each vial at different times. Collected samples were centrifuged at 10,000 rpm for 5 min using an OrtoAlresa Digicen 21R centrifuge to separate the solid phase. SAIL concentration was determined by UV absorption using an Agilent 8543 UV–visible absorption spectrophotometer. The equipment was previously calibrated at a wavelength of 259 nm (see Fig. S3 in SI). Adsorption density (mg/g_{rock}) was calculated by using the following equation:

$$Adsorption\ (\mathrm{mg/g}) = (C_0 - C)\frac{V}{m} \quad (2)$$

where C_0 is the initial surfactant concentration (mg/mL), C is the surfactant concentration at a certain time (mg/mL), V is the total volume of solution (mL), and m is the mass of crushed rock (g).

2.2.4. Contact angle measurements

The effect of the formulation on rock wettability was evaluated by measuring the contact angle between crude oil and rock surface in brine solution. To that aim, carbonate core plugs samples were sliced in 5 mm thickness discs. Experiments were carried out using the static sessile drop method according to previous literature (Roustaei and Bagherzadeh, 2015; Lara Orozco et al., 2020; Mohammadi and Riahi, 2020; Veiskarami et al., 2020). The experimental setup consists of a homemade glass cell with a holder to fix the plate rock sample. The glass cell is equipped with a septum in its lowest part to inject a drop of crude oil (6 μL).

Rock discs were first saturated in a brine solution for 24 h at room temperature. Afterwards, rock plates were immersed in crude oil for a period of 10 days at room temperature. Excess oil was removed from the discs, and they were immersed for 2 h in brine, surfactant, and nanofluid formulations, and contact angles were measured.

Additionally, an aging process to alter the original rock wettability towards oil-wet was carried out. After equilibration in brine (24 h), the rock discs were aged in crude oil for 10 days at 343.15 K. Excess oil was removed, then they were immersed for 2 h at the same temperature in brine or formulations, and contact angles were determined. All the measurements were repeated at least three times to ensure repeatability.

Wettability of the rock was classified as water-wet for contact angles from 0° to 75°, intermediate-wet from 75° to 105°, and oil-wet from 105° to 180° (Treiber and Owens, 1972).

2.2.5. Core flooding tests

Three core flooding experiments were conducted using a core-flooding system (Fig. 3) equipped with a Hassler core holder H00-021-0 and two piston pumps floXlab BTSP 500–5 provided by Vince Technologies. The piston pumps, equipped with pressure sensors, were used for the injection of crude oil or aqueous formulations. A confining pressure of ca. 60 bar was applied using a manual hydraulic pump Enerpac P142 to prevent hydraulic side flow. Three carbonate rocks of 3.8 cm diameter and 7.6 cm length were used for core flooding experiments. Graduated tubes were used to collect the effluent produced. Experiments were carried out at room temperature.

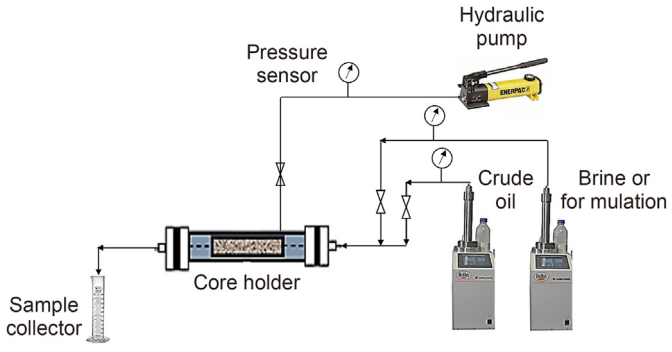

Fig. 3. Core-flooding experimental set-up.

The experimental procedure was based on previous literature (Bin Dahbag et al., 2015; Rodríguez-Palmeiro et al., 2017). The rock sample was introduced in the core holder and vacuumed for 24 h to evacuate the gas remaining inside the pores of the rock. In order to characterize the rock, the core was saturated with synthetic brine at a constant injection rate of 2 mL/min. After 24 h, the wet weight of the core was determined and used to calculate the pore volume (PV), as the difference between the dry and wet weights. The absolute permeability of the rock (k_w) was calculated using Darcy's law by recording the pressure difference (ΔP) between the inlet and outlet of the core at different injection flow rates.

The carbonate core was flooded with crude oil, displacing the brine contained in the pores, by gradually increasing the injection rate from 2 up to 10 mL/min, until there was no brine coming out from the effluent. The original oil in place (OOIP) was then calculated as the difference between incoming and exiting volumes of crude oil. Initial water saturation (S_{wi}) and initial oil saturation (S_{oi}) were calculated as the percentage of the PV occupied by brine and crude oil, respectively. Subsequently, the core was aged for 7 days at room temperature. When the aging was finished, the rock was flooded with synthetic brine at a constant injection rate of 2 mL/min. Brine injection was continued until reaching the residual oil saturation (S_{or}), calculated as the percentage of oil remaining in the core after conventional water flooding.

Several EOR or tertiary flooding extractions were conducted in order to check the performance of surfactant, surfactant-polymer and nanofluid formulations for EOR. The core was flooded with the different formulations at a constant flow rate of 2 mL/min until oil was no longer produced in the effluent. Additional oil recovery (AOR) was calculated as a function of the OOIP.

3. Results and discussion

3.1. Nanofluids preparation and characterization

3.1.1. Stability

In order to know the maximum concentration of Al_2O_3 nanoparticles that gave rise to stable nanofluids containing 0.01, 0.05, 0.1, 0.5 and 1.0 wt% of [C_{12}py]Cl in water, several mixtures were prepared with different concentrations of the nanomaterial at room conditions. The stability of the dispersion was examined by visual observation with time up to 7 days. After this time, stable nanofluids were whitish transparent solutions showing no precipitation. As an example, Fig. S4 shows dispersions of different Al_2O_3 concentrations in aqueous solution containing 0.05 wt% [C_{12}py]Cl (images taken 7 days after preparation). The absence of nanoparticles (Fig. S4a) gave rise to a clear solution. Concentrations of 0.05 and 0.1 wt% of Al_2O_3 (Figs. S4b and S4c) didn't show precipitation, and nanoparticle sedimentation is observed in the vial corresponding to a concentration of 1.5 wt% of Al_2O_3 (Fig. S4d).

Table 3 shows maximum concentration of Al_2O_3 nanoparticles in aqueous solutions of [C_{12}py]Cl, as a function of SAIL concentration, resulting in stable nanofluids. As shown, the highest nanoparticle concentration (3.0 wt%) was achieved at the lowest ionic liquid concentration (0.01 wt%). As the SAIL concentration

Table 3
Maximum concentration of nanoparticles in aqueous solutions of [C_{12}py]Cl, as a function of SAIL concentration, resulting in stable nanofluids.

[C_{12}py]Cl, wt%)	0.01	0.05	0.10	0.50	1.00
Al_2O_3, wt%)	3.00	1.00	0.05	0.02	0.01

increases, the maximum possible concentration of nanoparticles decreases. In fact, when [C_{12}py]Cl concentration is 1 wt%, concentrations of nanoparticles higher than 0.01 wt% give rise to precipitation. At the highest SAIL concentrations, the aggregation of nanoparticles is favored, the instability of the dispersion increases, and therefore precipitation occurs. As previously reported (Choudhary et al., 2017; Cacua et al., 2019), the alumina nanofluids with no added surfactant show better dispersion than those with surfactants. This is because alumina in polar liquids is able to develop a significant surface charge that enhances dispersion stability via electrostatic repulsion. In the case where Al_2O_3 nanoparticles are combined with the cationic SAIL [C_{12}py]Cl, the head group of the surfactant experiences a natural repulsion to the positively charged alumina surface, generating aggregation of the nanoparticles and destabilizing the nanofluid.

Zeta potential measurement was also carried out as a complementary tool to ensure the stability of the dispersions. For the dispersions of compositions shown in Table 3, all zeta-potential values were larger than 30 ± 5 mV. Moreover, no significant decrease in the zeta potential values was observed during the 7 monitored days. These results demonstrate that prepared nanofluids are stable or moderately stable suspensions (Hwang et al., 2008; Choudhary et al., 2017; Saha et al., 2018; Cacua et al., 2019; Pal et al., 2019).

As reservoirs usually contain brine, the stability of nanoparticles in the presence of NaCl was also analyzed. It was found that small amounts of the salt, even in trace amounts, broke the stability of the Al_2O_3 nanoparticles in the dispersion. This may be due to the decrease of the thick diffuse electrical layer of the nanoparticles, which is highly related to the concentration of salt in the medium (Liu et al., 2020; Rostami et al., 2020). As previously reported in the literature, to solve this problem of aggregation and deposition of nanoparticles, a stabilizing agent can be added. In this work, PVP was selected as a stabilizing agent. According to previous studies (Xia et al., 2014; Hendraningrat and Torsæter, 2015; Ali et al., 2018b), a concentration of 1.0 wt% of PVP was fixed for all the nanofluids containing NaCl. Thus, the stability of the nanoparticles in brine (0.5, 1.5 and 5.0 wt% NaCl) solutions containing 0.01, 0.05, 0.1, 0.5 and 1.0 wt% of [C_{12}py]Cl and 1.0 wt% of PVP was also determined. Results can be seen in Table 4. In this case, maximum concentration of nanoparticles increases with the increase of SAIL concentration and the reduction of NaCl concentration, 0.13 Al_2O_3 wt% being the maximum value achieved for solutions containing 1.0 wt% of [C_{12}py]Cl, 0.5 wt% NaCl and 1.0 wt% PVP (always considering stability after 7 days of preparation). The zeta potential

Table 4
Maximum concentration of nanoparticles in brine solutions of [C_{12}py]Cl, as a function of SAIL concentration, resulting in stable nanofluids. 1.0 wt% PVP was used as stabilizing agent.

[C_{12}py]Cl, wt%	Al_2O_3, wt%		
	0.5 wt% NaCl	1.5 wt% NaCl	5.0 wt% NaCl
0.01	0.10	0.075	0.05
0.05	0.10	0.075	0.05
0.10	0.10	0.075	0.05
0.50	0.10	0.075	0.05
1.00	0.13	0.10	0.05

of the stable samples was determined and values about 1 ± 0.5 mV were obtained. It has been previously reported that these zeta potential values are due to the presence of the polymer in the dispersion, the steric hindrance effect dominates over the electrostatic barrier effect, resulting in decreased zeta potential values (Pal et al., 2019).

3.1.2. Characterization

Density and viscosity measurements were carried out at 298.15 K and atmospheric pressure for stable nanofluids formulated in water. Results are shown in Table 5. Viscosity values are also represented in Fig. 4(a). In the range of concentrations tested, the influence of nanoparticle concentration is higher than SAIL concentration on physical properties. The increase in nanoparticle concentration increases both density and viscosity, more noticeably at low concentrations of the SAIL due to existence of stable nanofluids. As a higher concentration of nanoparticles was achieved with nanofluids containing 0.5 wt% NaCl than at other salt concentrations, density and viscosity was also determined for these nanofluids. Results are also shown in Table 5. As expected, the presence of PVP led to an increase in the fluid's viscosity (see Fig. 4(b)) that, as in the case of water, also increased with nanoparticle concentration. Thus, combining PVP and nanoparticles, viscosity values up to 1.55 mPa·s were achieved. This is significant from the point of view of EOR, since the increase in the viscosity of the displacing fluid avoids adverse mobility ratios and improves displacement efficiency.

3.2. Dynamic interfacial tension (IFT)

The SAIL [C_{12}py]Cl was selected in this work due to its interesting interfacial properties. A consistent value of CMC in water at 298.15 K was found in Literature. Measurements were carried out by Maeda and Sataki (1984) using ion-selective electrodes (16.3 mM), and by Galán et al. (2002) (~16.6 mM), Bhat et al. (2008) (16.2 mM) and Tennouga et al. (2015) (15.27 mM) using electrical conductivity. Both, Galán et al. (2002) and Tennouga et al. (2015) report a variation with temperature showing a minimum around 298 K due to hydrophobic interactions between the tails, and electrostatic repulsion between the ionic heads. Regarding the influence of salinity, it was found (Maeda and Sataki, 1984; Bhat et al., 2008) that CMC decreases with salt concentration due to the decrease of the electrostatic repulsion between the head groups of the SAIL.

With the aim of analyzing the ability of the SAIL [C_{12}py]Cl with and without nanoparticles to reduce water-oil IFT, dynamic interfacial tension measurements were carried out at 298.15 K. To check if the addition of nanoparticles would help to reduce IFT, measurements were first carried out in water. Three [C_{12}py]Cl solutions (0.1, 0.5 and 1 wt% SAIL) were prepared without nanoparticles and with 0.005 and 0.01 wt% Al_2O_3 (stable nanofluids in all the cases). Dynamic IFT curves can be seen in Figs. S5–S7 in SI, and equilibrium values are presented in Fig. 5 (IFT > 10 mN/m are outside the measurement range of the Spinning Drop instrument and were not determined). As expected, the presence of the surfactant led to a significative reduction of the IFT, this reduction being less appreciable at concentrations higher than 0.5 wt%. This is in agreement with the CMC values at 298.15 K published for this SAIL (Maeda and Sataki, 1984; Galán et al., 2002; Bhat et al., 2008; Tennouga et al., 2015). Fig. 5 also shows that the presence of nanoparticles helps to reduce IFT, the effect being obviously more noticeable at low concentrations of surfactant. This effect is generally found when nanofluids are used instead of surfactants (Kamal et al., 2017; Sun et al., 2017; Ali et al., 2018a; Cheraghian et al., 2020), since the presence of nanoparticles slightly decreases the water-oil IFT.

Table 5
Density and viscosity of nanofluids at 298.15 K and atmospheric pressure.

Nanofluids formulated in water				Nanofluids formulated in brine					
$[C_{12}py]Cl$, wt%	Al_2O_3, wt%	ρ, kg/m^3	η, mPa·s	$[C_{12}py]Cl$, wt%	Al_2O_3, wt%	PVP, wt%	NaCl, wt%	ρ, kg/m^3	η, mPa·s
0.011	0.000	997.5	0.90	0.011	0.000	1.000	0.500	1003.0	1.10
0.010	0.050	997.7	0.97	0.010	0.053	1.000	0.500	1003.2	1.18
0.011	0.102	998.1	1.12	0.010	0.101	0.998	0.515	1003.6	1.28
0.010	1.002	1006.1	1.99	–	–	–	–	–	–
0.049	0.000	997.3	0.90	0.051	0.000	1.000	0.505	1003.0	1.10
0.050	0.052	997.5	1.08	0.050	0.051	1.000	0.502	1003.2	1.27
0.051	0.101	997.9	1.17	0.050	0.100	1.000	0.500	1003.3	1.39
0.100	0.000	997.4	0.90	0.100	0.000	1.000	0.500	1003.0	1.11
0.100	0.005	997.4	0.94	0.100	0.051	1.000	0.500	1003.4	1.38
0.100	0.010	997.5	1.01	0.100	0.102	1.001	0.500	1003.7	1.44
0.500	0.000	997.4	0.91	0.499	0.000	1.000	0.500	1002.9	1.14
0.500	0.005	997.4	0.99	0.500	0.051	1.000	0.500	1003.3	1.42
0.500	0.011	997.5	1.07	0.500	0.101	1.000	0.500	1003.6	1.50
0.998	0.000	997.3	0.92	1.006	0.000	0.998	0.501	1003.2	1.16
1.000	0.005	997.4	1.09	1.000	0.050	1.000	0.501	1003.4	1.49
1.000	0.010	997.4	1.16	1.000	0.100	1.000	0.501	1003.8	1.55

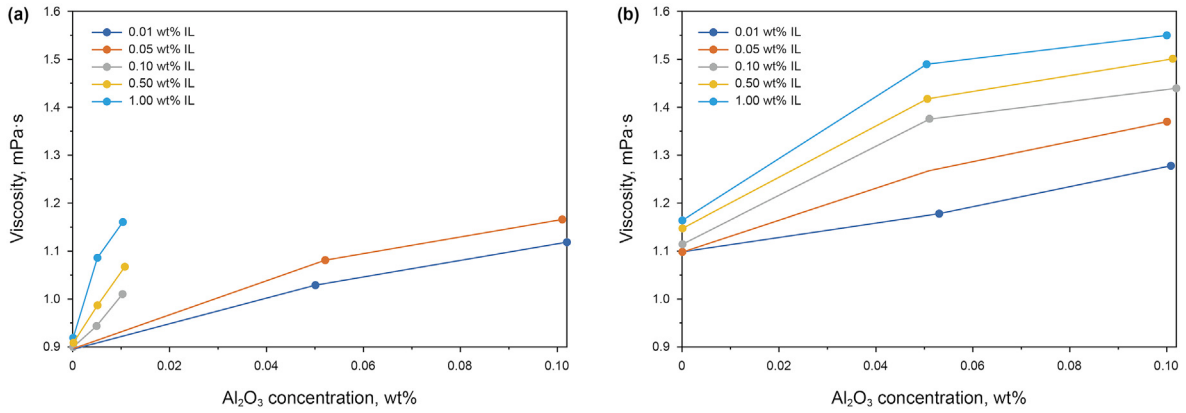

Fig. 4. Viscosity at 298.15 K and atmospheric pressure for stable nanofluids (see Table 5) in: (**a**) water, (**b**) brine. The lines are only drawn to facilitate visualization.

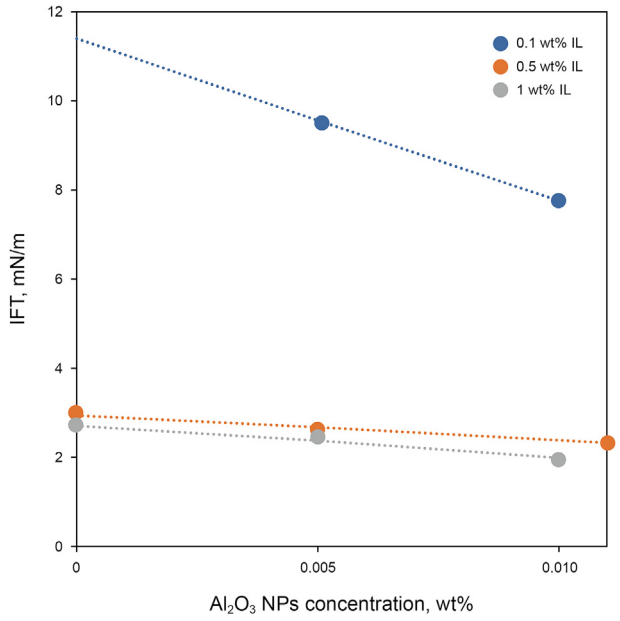

Fig. 5. Effect of $[C_{12}py]Cl$ and Al_2O_3 concentrations on equilibrated IFT between crude oil and water at 298.15 K and atmospheric pressure.

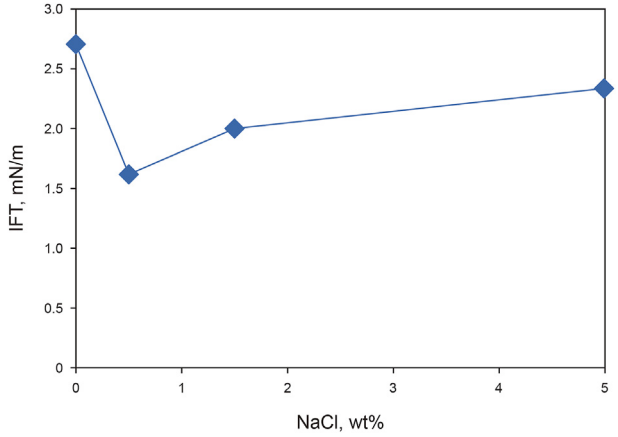

Fig. 6. Effect of NaCl concentrations on equilibrated IFT between crude oil and brine at 298.15 K and atmospheric pressure.

According to the results obtained in water, it can be stated that it is worth using nanoparticles to reduce IFT. However, as reservoirs usually contain salt, the influence of this addition was analyzed. To that aim, 1 wt% $[C_{12}py]Cl$ solution with different NaCl concentrations (from pure water to 5 wt% NaCl) were prepared and brine-oil IFT measured. Dynamic measurements can be seen in Fig. S8 (SI)

and equilibrated values are presented in Fig. 6. This figure shows that increasing the NaCl concentration from 0.0 to 0.5 wt%, IFT decreases from 2.7 to 1.6 mN/m. Nevertheless, when the concentration of NaCl is increased to 1.5 and 5 wt%, the IFT increases to 2.0 and 2.3 mN/m, respectively. Hezave et al. (2013) measured IFT for $[C_{12}py]Cl$ concentrations from 100 to 1000 ppm and NaCl concentrations from 15 to 30 wt%. They found that at those lower SAIL concentrations, NaCl concentration reduced IFT. Salts can reduce interfacial curvature by compressing the head group area of the surfactant molecules but, especially at high concentrations, may facilitate the surfactant's solubility in the oil phase through salting-out effect (Jia et al., 2017). At low NaCl concentration, salt ions neutralize the charges of the surfactant head groups and the IFT decreases. High salinity enhances the salting-out effect and the IFT increases. On the other hand, Hezave et al. (2013) also demonstrated a decrease in functionality of the SAIL when the temperature increases.

As 0.5 wt% NaCl led to the lowest IFT, this was selected as optimal salt concentration for the design of formulations, and the effect of nanoparticles and SAIL concentrations on brine-oil IFT was analyzed. To that aim, three $[C_{12}py]Cl$ solutions (0.1, 0.5 and 1 wt% SAIL) were prepared in brine (0.5 wt% NaCl) without nanoparticles and with 0.05 and 0.1 wt% Al_2O_3 (1 wt% PVP was used with nanoparticles to obtain stable nanofluids). Dynamic IFT curves can be seen in Figs. S9–S11 in SI, and equilibrium values are presented in Fig. 7. Similar behavior to that of water (Fig. 5) was found. SAIL concentrations higher than 0.5 wt% hardly produced higher reduction of the IFT, and the concentration of nanoparticles slightly reduced this property. As low concentrations of nanoparticles were used, the formation of a mixed layer with surfactants at the interface between the injected fluid and oil could be the reason for an increase of the interface and reduction of the IFT (Cheraghian and Hendraningrat, 2016; Cheraghian et al., 2020). However, this physical adsorption would be limited at high concentration of surfactant. The surfactant cost is high and IFT was not significantly reduced from 0.5 wt% to 1 wt%, so the first concentration was selected as optimal. Also the increase of nanoparticle concentration from 0.05 to 0.1 wt% hardly changed IFT (Fig. 6) or viscosity (Table 5), so the following nanofluid was selected as optimal: 0.05 wt% Al_2O_3, 1.0 wt% PVP, 0.5 wt% $[C_{12}py]Cl$, 0.5 wt% NaCl. The proposed nanofluid was not able to reach ultra-low IFT, however, the concentration of the surfactant in the injection fluid is low (a key factor for EOR formulations) and the synergy of the SAIL with the nanofluid facilitates other recovery mechanisms such as adsorption reduction or wettability alteration as will be shown in the next sections.

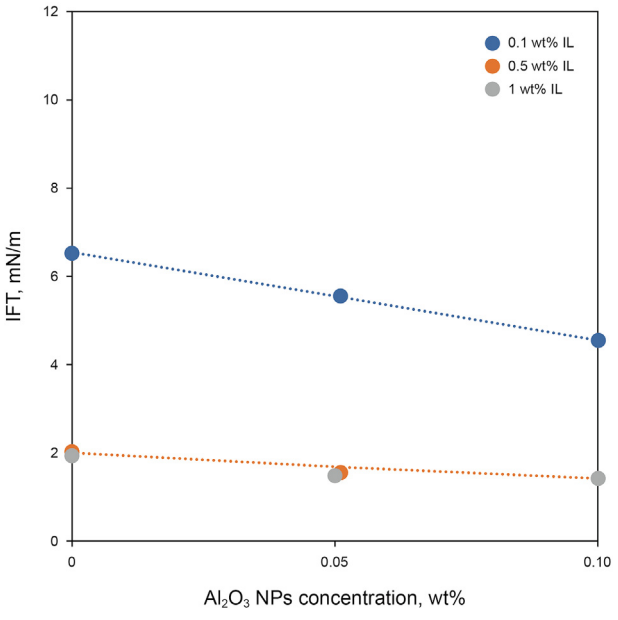

Fig. 7. Effect of $[C_{12}py]Cl$ and Al_2O_3 concentrations on equilibrated IFT between crude oil and brine (0.5 wt% NaCl) at 298.15 K and atmospheric pressure. Note: in the case of nanofluids 1 wt% PVP was used as stabilizing agent.

3.3. Adsorption studies

An important parameter to be evaluated before carrying out an EOR operation is the possible adsorption of the surfactant in the reservoir rock. For this reason, the adsorption of the proposed nanofluid was studied on sandstone and carbonate rocks via batch experiments. For comparative purposes, the adsorption of the surfactant formulation (without nanoparticles) was also studied.

Fig. 8 shows the adsorption of the surfactant formulation (0.5 wt % $[C_{12}py]Cl$, 0.5 wt% NaCl) in sandstone and carbonate rocks. As expected, the adsorption of the cationic surfactant is excessively high (7.98 mg/g at equilibrium) in sandstone rock. Adsorption of surfactants is mainly due to the electrostatic attraction between the charged head group of the surfactant and charged surface of the rock (Hanamertani et al., 2018). Sandstone cores are composed of silicate-like minerals (albite and muscovite) that are negatively charged at neutral pH or in water (Bera et al., 2013), and $[C_{12}py]Cl$ is a cationic surfactant, so the result was foreseeable. Conversely, the surface of carbonate cores is positively charged due to the presence of calcite and other minerals containing Mg^{2+} (Tagavifar et al., 2017), thus repulsive interactions with the head of the SAIL led to a significative lower adsorption at equilibrium (2.56 mg/g). The presence of nanoparticles is capable of reducing the surfactant or polymer adsorption on the rock surface (Kamal et al., 2017; Li et al., 2018; Afolabi, 2019). The adsorption of the nanofluid formulation (0.05 wt% Al_2O_3, 1.0 wt% PVP, 0.5 wt% $[C_{12}py]Cl$, 0.5 wt% NaCl), on the two crushed rocks, showed a similar trend to that observed in the surfactant formulations with a slight improvement (Fig. 8). Adsorption in sandstone rocks was reduced to 7.54 mg/g (still large enough to render the process unfeasible) and in the case of carbonate rocks to 2.23 mg/g. Therefore, the carbonate rock was selected to perform contact angle and core flooding tests.

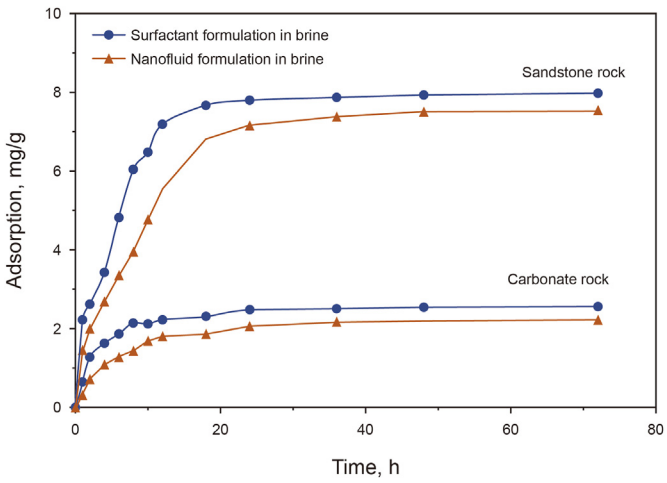

Fig. 8. Evolution of the surfactant adsorption in sandstone and carbonate rocks with time.

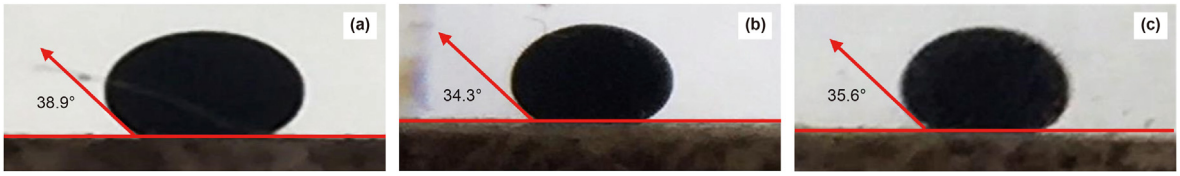

Fig. 9. Contact angle measurements after aging 10 days at room temperature: (**a**) brine, (**b**) surfactant formulation, (**c**) nanofluid formulation.

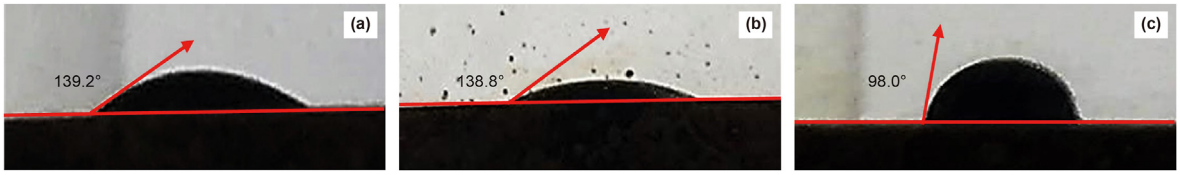

Fig. 10. Contact angle measurements after aging 10 days at 343.15 K: (**a**) brine, (**b**) surfactant formulation, (**c**) nanofluid formulation.

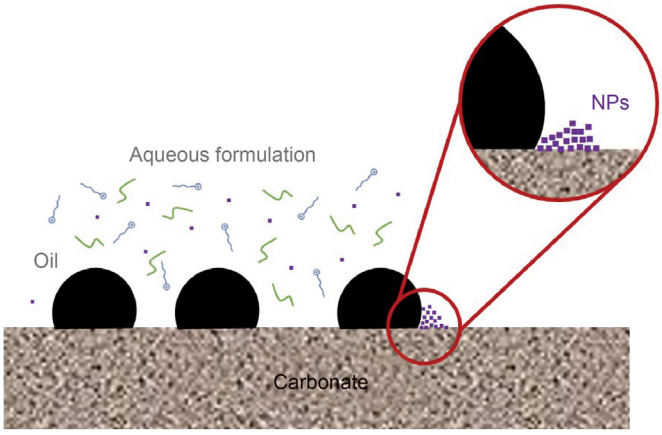

Fig. 11. Wettability alteration by nanoparticles.

3.4. Contact angle measurements

Wettability is another key parameter in oil recovery processes and reservoir productivity. The literature shows that the presence of nanoparticles in aqueous solutions can switch the wettability of rocks from oil-wet towards water-wet (Ebrahim et al., 2019; Gbadamosi et al., 2019; Asl et al., 2020; Habibi et al., 2020). In this work, to evaluate the effect of nanoparticles on the wettability of carbonate rocks, different experiments were carried out. Fig. 9 shows results obtained when the carbonate rock was aged 10 days at room conditions. Initial contact angle (38.9°) was reduced to 34.3° and 35.6° when the rock was treated with the surfactant (0.5 wt% [C_{12}py]Cl, 0.5 wt% NaCl) and nanofluid (0.05 wt% Al_2O_3, 1.0 wt% PVP, 0.5 wt% [C_{12}py]Cl, 0.5 wt% NaCl) formulations, respectively. No change was observed in the rock wettability, being water-wet in all the cases.

Fig. 10 shows results obtained when the carbonate rock was aged 10 days at 343.15 K. In this case, initial rock wettability was oil-wet with a contact angle of 139.2°. When the rock was treated with the surfactant and nanofluid formulations, obtained contact angles after 2 h were 138.8° and 98.0°, respectively. The surfactant formulation was not able to change the wettability whilst the nanofluid changed it to intermediate-wet. Mohammadi et al. (2014) showed, using scanning electron microscopy, that Al_2O_3 nanoparticles generated nanostructures on the surface of carbonate rocks. These ordered structures are located near the three-phase contact line (wetting wedge) of a drop or bubble on a solid surface, promoting the spreading of the nanofluid and making the system more water-wet (Wasan et al., 2011). Fig. 11 shows this mechanism.

3.5. Core flooding experiments

Core-flooding tests were carried out at room conditions in carbonate cores (details are shown in Table 6) with surfactant and nanofluid formulations. In order to check the effect of the polymer, a test was also developed with the surfactant solution and PVP but without nanoparticles. Injected Pore Volumes (PV) of the different chemical slugs were the required until no more oil was extracted. Test 1 (see Table 6) was conducted with the surfactant formulation. After secondary flooding, 2.7 PV of formulation were injected leading to an additional oil recovery (AOR) of 3.39% OOIP. When PVP was added to the formulation, 3.9 PV of injected chemical slug led to an AOR of 7.39% of OOIP. Test 3 shows the results with the nanofluid formulation, 3.7 PV of injection allowed an AOR of 11.96% OOIP.

Nanofluid formulation led to the highest oil recovery. The mechanisms involved are adsorption and IFT reduction and viscosity increase. Moreover, as previously shown, the presence of nanoparticles weakens the mobility of the polymer molecules (Gbadamosi et al., 2019), helping EOR. It is worth mentioning that, due to the limitations in the experimental configuration of the core holder, flooding tests were carried out at water-wet rock conditions. However, it was shown (section 3.3) that the nanofluid formulation can also produce wettability change as another oil recovery mechanism.

Table 7 shows our results compared with previously proposed formulations containing surfactants and nanoparticles for EOR in carbonate reservoirs. It can be seen that our results are either similar to, or clearly better than previous studies. The only exception is the work of Liu et al. (2021) who proposes a chemical slug containing laurel anolamide and amine-terminated silica nanoparticles. However, the proposed formulation requires a clearly higher concentration of chemicals and the synthesis of functionalized nanoparticles. Moreover, the authors do not present adsorption studies.

4. Conclusions

In this work, the advantages of mixing nanoparticles and SAILs

Table 6
Summary of core flooding experiments.

	Test 1	Test 2	Test 3
Porosity of the core, %	18.29	14.68	18.08
Permeability, mD	34.19	15.88	22.02
Pore volume, mL	15.37	12.66	15.71
OOIP, mL	8.85	8.80	9.2
Initial oil saturation, %	57.57	69.53	58.56
Initial water saturation, %	42.43	30.47	41.44
Oil recovered after brine (0.5 wt% NaCl) flooding, % OOIP	66.67	67.04	58.70
Residual oil saturation, %	19.19	22.91	24.19
Chemical slug injected	2.7 PV of 0.5 wt% [C_{12}py]Cl	3.9 PV of 0.5 wt% [C_{12}py]Cl + 1 wt% PVP	3.7 PV of 0.05 wt% Al_2O_3 + 1 wt% PVP + 0.5 wt% [C_{12}py]Cl
Additional Oil Recovered during chemical flooding, % OOIP	3.39	7.39	11.96

Table 7
Comparison with previous studies with nanofluids containing surfactants in carbonate rocks.

Author	Nanofluid formulation	Rock properties	Brine Composition	Temperature	IFT, mN/m	Adsorption, mg/g rock	AOR, % OOIP
Khademolhosseini et al. (2019)	97.5 ppm of hydrophilic silica NPs, 110.8 ppm of rhamnolipid BS and 1.17 wt % NaCl	ø: 14.1% μ: 1.45 mD	3 wt% NaCl	Room temperature	1.85	Not determined	5.1
Liu et al. (2021)	500 ppm of mine-terminated silica NPs and 4000 ppm of laurel anolamide	ø: 17.6% μ: 50/100/300 mD	1.87% TDS	30 °C	0.075	Not determined	29.2
Rezaei et al. (2020a)	1000 ppm of alpha olephin sulphonate (AOS) and 1000 ppm hydrophilic silica NPs	ø: 13–17% μ: 1.05–1.51 mD	18 wt% NaCl	Room temperature	4.4	Not determined	8.6
Rezaei et al. (2020b)	250 ppm of cocamidopropyl betaine (CAPB) and 1000 ppm of silica NPs	ø: 19–22% μ: 8–10 mD	FW: 19.8 wt % NaCl SSW: 5 wt% NaCl	Room temperature	0.98	0.511	12.2
Present work	5000 ppm of 1-dodecylpyridinium chloride, 10,000 ppm of polyvinylpyrrolidone and 500 ppm of aluminium oxide NPs	ø: 14–18% μ: 15–34 mD	0.5 wt% NaCl	Room temperature	1.56	2.23	11.96

for EOR were explored. Namely, several nanofluids constituted of Al_2O_3 nanoparticles and the SAIL [C_{12}py]Cl were prepared, characterized and tested for EOR. From this work, several conclusions may be established:

- The stability of the nanofluid is likely the bottleneck of the application. The concentration of nanoparticles that form stable nanofluids for long periods of time is low, practically null in the case of formulations designed in brine, as practical application usually requires.
- The polymer PVP can be used as stabilizing agent. Using formulations with 1 wt% PVP, Al_2O_3 concentration up to 0.1 wt% could be achieved depending on SAIL and NaCl concentration.
- When Al_2O_3 nanoparticles and PVP as stabilizing agent are added to brine solutions of [C_{12}py]Cl, the viscosity increases, thereby offering a combination of methods (surfactant-polymer) for EOR.
- The presence of nanoparticles slightly improves the reduction of the water-oil IFT achieved with the SAIL, and reduces the surfactant adsorption on carbonate rocks (high adsorption in sandstone, with or without nanoparticles, makes use with these rocks impractical).
- Based on IFT reduction, a surfactant (0.5 wt% [C_{12}py]Cl, 0.5 wt% NaCl) and a nanofluid (0.05 wt% Al_2O_3, 1.0 wt% PVP, 0.5 wt% [C_{12}py]Cl, 0.5 wt% NaCl) formulations were designed and tested for EOR through flooding experiments. The nanofluid formulation is the best option for EOR, with an AOR of 11.96% OOIP, improving results obtained with surfactant alone or surfactant-polymer flooding.
- The nanofluid formulation is also able to change wettability from oil-wet to intermediate-wet.

Acknowledgements

The authors acknowledge the Ministry of Science and Innovation and State Research Agency for financial support throughout project PGC2018-097342-B-I00, including European Regional Development Fund A. Al-Asadi acknowledges Sothern Technical University for financial support. We would also like to thank Repsol (A Coruña) for providing the crude oil used for the experiments.

Appendix A. Supplementary data

Supplementary data to this article can be found online at https://doi.org/10.1016/j.petsci.2022.08.018.

References

Afolabi, R.O., 2019. Enhanced oil recovery for emergent energy demand: challenges and prospects for a nanotechnology paradigm shift. Int. Nano Lett. 9, 1–15. https://doi.org/10.1007/s40089-018-0248-0.
Ahmadi, M.A., Zendehboudi, S., Shafiei, A., James, L., 2012. Nonionic surfactant for enhanced oil recovery from carbonates: adsorption kinetics and equilibrium. In: Eng. Chem. Res., vol. 51, pp. 9894–9905. https://doi.org/10.1021/ie300269c.
Ahmadi, M.A., Shadizadeh, S.R., 2015. Experimental investigation of a natural surfactant adsorption on shale-sandstone reservoir rocks: static and dynamic conditions. Fuel 159, 15–26. https://doi.org/10.1016/j.fuel.2015.06.035.
Ahmadi, M.A., 2016. Use of nanoparticles to improve the performance of sodium dodecyl sulfate flooding in a sandstone reservoir. Europ. Phys. J. Plus. 131, 435. https://doi.org/10.1140/epjp/i2016-16435-5.
Ahmadi, M.A., Shadizadeh, S.R., 2019. Spotlight on the new natural surfactant

flooding in carbonate rock samples in low salinity condition. Sci. Rep. 8, 10985. https://doi.org/10.1038/s41598-018-29321-w.
Ali, J.A., Kolo, K., Manshad, A.K., Mohammadi, A.H., 2018a. Recent advances in application of nanotechnology in chemical enhanced oil recovery: effects of nanoparticles on wettability alteration, interfacial tension reduction, and flooding. Egyp. J. Petrol. 27 (4), 1371–1383. https://doi.org/10.1016/j.ejpe.2018.09.006.
Ali, N., Teixeira, J.A., Addali, A., 2018b. A review on nanofluids: fabrication, stability, and thermophysical properties. J. Nanomater. 6978130. https://doi.org/10.1155/2018/6978130.
Al-Wahaibi, Y., Al-Hashmi, A.A., Joshi, S., Mosavat, N., Rudyk, S., Al-Khamisi, S., Al-Kharusi, T., Al-Sulaimani, H., 2017. Mechanistic study of surfactant/polymer adsorption and its effect on surface morphology and wettability. In: Paper Presented at the SPE Oil and Gas India Conference and Exhibition. Mumbai, India, April. https://doi.org/10.2118/185327-MS.
Asl, H.F., Zargar, G., Manshada, A.K., Takassi, M.A., Ali, J.A., Keshavarze, A., 2020. Effect of SiO_2 nanoparticles on the performance of L-Arg and L-Cys surfactants for enhanced oil recovery in carbonate porous media. J. Mol. Liq. 300, 112290. https://doi.org/10.1016/j.molliq.2019.112290.
Bera, A., Kumar, T., Ojha, K., Mandal, A., 2013. Adsorption of surfactants on sand surface in enhanced oil recovery: isotherms, kinetics and thermodynamic studies. Appl. Surf. Sci. 284, 87–99. https://doi.org/10.1016/j.apsusc.2013.07.029.
Bera, A., Belhaj, H., 2016. Ionic liquids as alternatives of surfactants in enhanced oil recovery—a state-of-the-art review. J. Mol. Liq. 224, 177–188. https://doi.org/10.1016/j.molliq.2016.09.105.
Bhat, M.A., Dar, A.A., Amin, A., Rather, G.M., 2008. Co- and counterion effect on the micellization characteristics of dodecylpyridinium chloride. J. Dispersion Sci. Technol. 29, 514–520. https://doi.org/10.1080/01932690701728841.
Bin Dahbag, M., AlQuraishi, A., Benzagouta, M., 2015. Efficiency of ionic liquids for chemical enhanced oil recovery. J. Pet. Explor. Prod. Technol. 5, 353–361. https://doi.org/10.1007/s13202-014-0147-5.
Cacua, K., Ordoñez, F., Zapata, C., Herrera, B., Pabón, E., Buitrago-Sierra, R., 2019. Surfactant concentration and pH effects on the zeta potential values of alumina nanofluids to inspect stability. Colloids Surf., A 583, 123960. https://doi.org/10.1016/j.colsurfa.2019.123960.
Cheraghian, G., Hendraningrat, L., 2016. A review on applications of nanotechnology in the enhanced oil recovery part A: effects of nanoparticles on interfacial tension. Int. Nano Lett. 6, 129–138. https://doi.org/10.1007/s40089-015-0173-4.
Cheraghian, G., Rostami, S., Afrand, M., 2020. Nanotechnology in enhanced oil recovery. Processes 8, 1073. https://doi.org/10.3390/pr8091073.
Choudhary, R., Khurana, D., Kumar, A., Subudhi, S., 2017. Stability analysis of Al_2O_3/water nanofluids. J. Exp. Nanosci. 12 (1), 140–151. https://doi.org/10.1080/17458080.2017.1285445.
Ebrahim, T., Mohsen, V.S., Mahdi, S.M., Esmaeel, K.T., Saeb, A., 2019. Performance of low-salinity water flooding for enhanced oil recovery improved by SiO_2 nanoparticles. Petrol. Sci. 16 (2), 357–365. https://doi.org/10.1007/s12182-018-0295-1.
Galán, J.J., González-Pérez, A., Del Castillo, J.L., Rodríguez, J.R., 2002. Thermal parameters associated to micellization of dodecylpyridinium bromide and chloride in aqueous solution. J. Therm. Anal. Calorim. 70, 229–234. https://doi.org/10.1023/A:1020678222376.
Gangwar, J., Gupta, B.K., Kumar, P., Tripathi, S.K., Srivastava, A.K., 2014. Time-resolved and photoluminescence spectroscopy of θ-Al2O3 nanowires for promising fast optical sensor applications. Dalton Trans. 43, 17034. https://doi.org/10.1039/c4dt01831a.
Gbadamosi, A.O., Junin, R., Manan, M.A., Agi, A., Oseh, J.O., Usman, J., 2019. Synergistic application of aluminium oxide nanoparticles and oilfield polyacrylamide for enhanced oil recovery. J. Petrol. Sci. Eng. 182, 106345. https://doi.org/10.1016/j.petrol.2019.106345.
Habibi, S., Jafari, A., Fakhroueian, Z., 2020. Wettability alteration analysis of smart water/novel functionalized nanocomposites for enhanced oil recovery. Petrol. Sci. 17 (5), 1318–1328. https://doi.org/10.1007/s12182-020-00436-y.
Hanamertani, A.S., Pilus, R.M., Kamal Idris, A., Irawan, S., Tan, I.M., 2018. Ionic liquids as a potential additive for reducing surfactant adsorption onto crushed Berea sandstone. J. Petrol. Sci. Eng. 162, 480–490. https://doi.org/10.1016/j.petrol.2017.09.077.
Haruna, M.A., Gardy, J., Yao, G., Hu, Z., Hondow, N., Wen, D., 2020. Nanoparticle modified polyacrylamide for enhanced oil recovery at harsh conditions. Fuel 268, 117186. https://doi.org/10.1016/j.fuel.2020.117186.
Hendraningrat, L., Torsæter, O., 2015. Metal oxide-based nanoparticles: revealing their potential to enhance oil recovery in different wettability systems. Appl. Nanosci. 5, 181–199. https://doi.org/10.1007/s13204-014-0305-6.
Hezave, A.Z., Dorostkar, S., Ayatollahi, S., Nabipour, M., Hemmateenejad, B., 2013. Effect of different families (imidazolium and pyridinium) of ionic liquids-based surfactants on interfacial tension of water/crude oil system. Fluid Phase Equil. 360, 139–145. https://doi.org/10.1016/j.fluid.2013.09.025.
Hirasaki, G.J., Miller, C.A., Puerto, M., 2011. Recent advances in surfactant EOR. SPE J. 16 (4), 889–907. https://doi.org/10.2118/115386-PA.
Hwang, Y., Lee, J.K., Lee, J.K., Jeong, Y.M., Cheong, S.I., Ahn, Y.C., Kim, S.H., 2008. Production and dispersion stability of nanoparticles in nanofluids. Powder Technol. 186 (2), 145–153. https://doi.org/10.1016/j.powtec.2007.11.020.
Jia, H., Leng, X., Hu, M., Song, Y., Wu, H., Lian, P., Liang, Y., Zhu, Y., Liu, J., Zhou, H., 2017. Systematic investigation of the effects of mixed cationic/anionic surfactants on the interfacial tension of a water/model oil system and their application to enhance crude oil recovery. Colloids Surf., A 529, 621–627. https://doi.org/10.1016/j.colsurfa.2017.06.055.
Kamal, M.S., Adewunmi, A.A., Sultan, A.S., Al-Hamad, M.F., Mehmood, U., 2017. Recent advances in nanoparticles enhanced oil recovery: rheology, interfacial tension, oil recovery, and wettability alteration. J. Nanomater. 2473175. https://doi.org/10.1155/2017/2473175.
Khademolhosseini, R., Jafari, A., Mousavi, S.M., Manteghian, M., 2019. Investigation of synergistic effects between silica nanoparticles, biosurfactant and salinity in simultaneous flooding for enhanced oil recovery. RSC Adv. 9, 20281–20294. https://doi.org/10.1039/c9ra02039j.
Lara Orozco, R.A., Abeykoon, G.A., Wang, M., Argüelles-Vivas, F., Okuno, R., Lake, L.W., Ayirala, S.C., AlSofi, A.M., 2020. Amino acid as a novel wettability modifier for enhanced waterflooding in carbonate reservoirs. SPE Reservoir Eval. Eng. 23, 741–757. https://doi.org/10.2118/195907-PA.
Li, K., Wang, D., Jiang, S., 2018. Review on enhanced oil recovery by nanofluids. Oil Gas Sci. Technol. 73, 37. https://doi.org/10.2516/ogst/2018025.
Liu, Z., Bode, V., Hadayati, P., Onay, H., Sudhölter, E.J.R., 2020. Understanding the stability mechanism of silica nanoparticles: the effect of cations and EOR chemicals. Fuel 280, 118650. https://doi.org/10.1016/j.fuel.2020.118650.
Liu, R., Lu, J., Pu, W., Xie, Q., Lu, Y., Du, D., Yang, X., 2021. Synergetic effect between in-situ mobility control and micro-displacement for chemical enhanced oil recovery (CEOR) of a surface-active nanofluid. J. Pet. Sci. Eng. 205, 108983. https://doi.org/10.1016/j.petrol.2021.108983.
Maeda, T., Sataki, I., 1984. The micellar properties of 1-dodecylpyridinum chloride as studied by ion-selective electrodes. Bull. Chem. Soc. Jpn. 57, 2396–2399. https://doi.org/10.1246/bcsj.57.2396.
Mahmoudpour, M., Pourafshary, P., 2021. Investigation of the effect of engineered water/nanofluid hybrid injection on enhanced oil recovery mechanisms in carbonate reservoirs. J. Pet. Sci. Eng. 196, 107662. https://doi.org/10.1016/j.petrol.2020.107662.
Manshad, A.K., Rezaei, M., Moradi, S., Nowrouzi, I., Mohammadi, A.H., 2017. Wettability alteration and interfacial tension (IFT) reduction in enhanced oil recovery (EOR) process by ionic liquid flooding. J. Mol. Liq. 248, 153–162. https://doi.org/10.1016/j.molliq.2017.10.009.
Mohammadi, M.S., Moghadasi, J., Naseri, S., 2014. An experimental investigation of wettability alteration in carbonate reservoir using γ-Al_2O_3 nanoparticles. Iran. J. Oil & Gas Sci. Technol. 3, 18–26. https://doi.org/10.22050/IJOGST.2014.6034.
Mohammadi, M., Riahi, S., 2020. Experimental investigation of water incompatibility and rock/fluid and fluid/fluid interactions in the absence and presence of scale inhibitors. SPE J. 25 (5), 2615–2631. https://doi.org/10.2118/201117-PA.
Pal, N., Kumar, N., Saw, R.K., Mandal, A., 2019. Gemini surfactant/polymer/silica stabilized oil-in-water nanoemulsions: design and physicochemical characterization for enhanced oil recovery. J. Pet. Sci. Eng. 183, 106464. https://doi.org/10.1016/j.petrol.2019.106464.
Pal, N., Mandal, A., 2020. Enhanced oil recovery performance of gemini surfactant-stabilized nanoemulsions functionalized with partially hydrolyzed polymer/silica nanoparticles. Chem. Eng. Sci. 226, 115887. https://doi.org/10.1016/j.ces.2020.115887.
Rezaei, A., Abdollahi, H., Derikvand, Z., Hemmati-Sarapardeh, A., Mosavi, A., Nabipour, N., 2020a. Insights into the effects of pore size distribution on the flowing behavior of carbonate rocks: linking a nano-based enhanced oil recovery method to rock typing. Nanomaterials 10, 972. https://doi.org/10.3390/nano10050972.
Rezaei, A., Riazi, M., Escrochi, M., Elhaei, R., 2020b. Integrating surfactant, alkali and nano-fluid flooding for enhanced oil recovery: a mechanistic experimental study of novel chemical combinations. J. Mol. Liq. 308, 113106. https://doi.org/10.1016/j.molliq.2020.113106.
Rodríguez-Palmeiro, I., Rodríguez-Escontrela, I., Rodríguez, O., Soto, A., Reichmann, S., Amro, M.M., 2017. Tributyl(tetradecyl)phosphonium chloride ionic liquid for surfactant-enhanced oil recovery. Energy Fuel. 31, 6758–6765. https://doi.org/10.1021/acs.energyfuels.7b00544.
Rostami, P., Sharifi, M., Aminshahidy, B., Fahimpour, J., 2020. Enhanced oil recovery using silica nanoparticles in the presence of salts for wettability alteration. J. Dispersion Sci. Technol. 41 (3), 402–413. https://doi.org/10.1080/01932691.2019.1583575.
Roustaei, A., Bagherzadeh, H., 2015. Experimental investigation of SiO_2 nanoparticles on enhanced oil recovery of carbonate reservoirs. J. Pet. Explor. Prod. Technol. 5, 27–33. https://doi.org/10.1007/s13202-014-0120-3.
Saha, R., Uppaluri, R.V.S., Tiwari, P., 2018. Silica nanoparticle assisted polymer flooding of heavy crude oil: emulsification, rheology, and wettability alteration characteristics. Ind. Eng. Chem. Res. 57, 6364–6376. https://doi.org/10.1021/acs.iecr.8b00540.
Sharma, T., Kumar, G.S., Sangwai, J.S., 2015. Comparative effectiveness of production performance of Pickering emulsion stabilized by nanoparticle–surfactant–polymer over surfactant–polymer (SP) flooding for enhanced oil recovery for Brownfield reservoir. J. Pet. Sci. Eng. 129, 221–232. https://doi.org/10.1016/j.petrol.2015.03.015.
Sheng, J.J., 2011. Modern Chemical Enhanced Oil Recovery. Theory and Practice Elsevier, Amsterdam. https://doi.org/10.1016/C2009-0-20241-8, 2011.
Somasundaran, P., Zhang, L., 2006. Adsorption of surfactants on minerals for wettability control in improved oil recovery processes. J. Petrol. Sci. Eng. 52, 198–212. https://doi.org/10.1016/j.petrol.2006.03.022.
Somoza, A., Arce, A., Soto, A., 2022. Oil recovery tests with ionic liquids: a review and evaluation of 1-decyl-3-methylimidazolium triflate. Petrol. Sci. 19 (4),

1877–1887. https://doi.org/10.1016/j.petsci.2021.10.025.
Sun, X., Zhang, Y., Chen, G., Gai, Z., 2017. Application of nanoparticles in enhanced oil recovery: a critical review of recent progress. Energies 10, 345. https://doi.org/10.3390/en10030345.
Tagavifar, M., Jang, S.H., Sharma, H., Wang, D., Chang, L.Y., Mohanty, K., Pope, G.A., 2017. Effect of pH on adsorption of anionic surfactants on limestone: experimental study and surface complexation modeling. Colloids Surf., A 538, 549–558. https://doi.org/10.1016/j.colsurfa.2017.11.050.
Tennouga, L., Mansri1, A., Medjahed, K., Chetouani, A., Warad, I., 2015. The micelle formation of cationic and anionic surfactants in aqueous medium: determination of CMC and thermodynamic parameters at different temperatures. J. Mater. Environ. Sci. 6, 2711–2716.
Treiber, L.E., Owens, W.W., 1972. A laboratory evaluation of the wettability of fifty oil-producing reservoirs. Soc. Petrol. Eng. J. 12, 531–540. https://doi.org/10.2118/3526-PA.
Veiskarami, S., Jafari, A., Soleymanzadeh, A., 2020. Phase behavior, wettability alteration, and oil recovery of low-salinity surfactant solutions in carbonate reservoirs. SPE J. 25 (4), 1784–1802. https://doi.org/10.2118/200483-PA.
Wasan, D., Nikolov, A., Kondiparty, K., 2011. The wetting and spreading of nanofluids on solids: role of the structural disjoining pressure. Curr. Opin. Colloid In. 16 (4), 344–349. https://doi.org/10.1016/j.cocis.2011.02.001.
Xia, G., Jiang, H., Liu, R., Zhai, Y., 2014. Effects of surfactant on the stability and thermal conductivity of Al_2O_3/de-ionized water nanofluids. Int. J. Therm. Sci. 84, 118–124. https://doi.org/10.1016/j.ijthermalsci.2014.05.004.
Zabihi, S., Faraji, D., Rahnama, Y., Hezave, A.Z., Ayatollahi, S., 2019. Relative permeability measurement in carbonate rocks, the effects of conventional surfactants vs. Ionic liquid-based surfactants. J. Dispersion Sci. Technol. 41 (12), 1797–1811. https://doi.org/10.1080/01932691.2019.1637262.